

# On the formation of massive stars by accretion

P. Norberg<sup>1</sup> and A. Maeder<sup>2</sup>

<sup>1</sup> Department of Physics, University of Durham, Durham DH1 3LE, UK

<sup>2</sup> Observatoire de Genève, 1290 Sauverny, Switzerland

Received 2 February 2000 / Accepted 18 May 2000

**Abstract.** At present, there are two scenarios for the formation of massive stars: 1) The accretion scenario and 2) The coalescence scenario, which implies the merging of intermediate mass stars. We examine here some properties of the first one. Radio and IR observations by Churchwell (1999) and Henning et al. (2000) of mass outflows around massive Pre-Main Sequence (PMS) stars show an increase by several orders of magnitudes of the outflow rates with stellar luminosities, and thus with stellar masses. As typically, a fraction of  $\frac{1}{3}$  to  $\frac{1}{6}$  of the infalling material is estimated to be accreted, this suggests that the accretion rate is also quickly increasing with the stellar mass.

We calculate three different sets of birthlines, i.e. tracks followed by a continuously accreting star. First, three models with a constant accretion rate ( $\dot{M}_{\text{accr}} = 10^{-6}, 10^{-5}, 10^{-4} M_{\odot} \text{ yr}^{-1}$ ). Then several birthlines following the accretion models of Bernasconi & Maeder (1996), which have  $\dot{M}_{\text{accr}}$  increasing only slightly with mass. Finally we calculate several birthlines for which  $\dot{M}_{\text{accr}} = \dot{M}_{\text{ref}} \left( \frac{M}{M_{\odot}} \right)^{\varphi}$ , with values of  $\varphi$  equal to 0.5, 1.0 and 1.5 and also for different values of  $\dot{M}_{\text{ref}}$ . The best fit to the observations of PMS stars in the HR diagram is achieved for  $\varphi$  between 1.0 or 1.5 and for  $\dot{M}_{\text{ref}} \simeq 10^{-5} M_{\odot} \text{ yr}^{-1}$ . Considerations on the lifetimes favour values of  $\varphi$  equal to 1.5. These accretion rates do well correspond to those derived from radio and IR observations of mass outflows. Moreover they also lie in the “permitted region” of the dynamical models given by Wolfire & Cassinelli (1987).

We emphasize the importance of the accretion scenario for shaping the IMF, and in particular for determining the upper mass limit of stars. In the accretion scenario, this upper mass limit will be given by the mass for which the accretion rate is such that the accretion induced shock luminosity is of the order of the Eddington luminosity.

**Key words:** accretion, accretion disks – stars: evolution – stars: pre-main sequence

## 1. Introduction

The formation of massive stars is still a very uncertain domain of stellar astrophysics. Schematically, there are at present two very

different scenarios. 1) *The coalescence scenario* proposed by Bonnell et al. (1998) and Stahler et al. (2000). The formation of massive stars ( $M \geq 10M_{\odot}$ ) is assumed to occur by coalescence of stars of intermediate masses, which form through accretion onto initially lower mass protostars. The basic reason for the development of this formation scenario was the difficulty of accreting mass onto very luminous stars. 2) *The accretion scenario* was initially proposed by Stahler et al. (1980a, 1980b, 1981) and was further developed for low and intermediate mass stars (see for example Palla & Stahler, 1993). It was then investigated as a formation mechanism for massive stars by Beech & Mitalas (1994), Bernasconi & Maeder (1996). In this scenario, the massive stars no longer cross horizontally the HR diagram, coming from the red to the blue, on the Kelvin-Helmholtz timescale, but rise upwards in the HR diagram along the so-called birthline. The birthline is defined as the path in the HR diagram followed by a continuously accreting star. For low and intermediate mass stars, the birthline forms an upper envelope of individual evolutionary tracks in the HR diagram. The location of the birthline and the timescales on it strongly depend on the accretion rates  $\dot{M}_{\text{accr}}$  (Bernasconi & Maeder, 1996; Tout et al. 1999). Thus, in this scenario it is very important to know how the accretion rate varies with the mass already accreted onto the star.

Both scenarios have their own advantages and difficulties. They both influence the upper limit of stellar masses, but the physical mechanism determining this limit is of course different for each of the two above scenarios. In this paper we shall examine some properties of the accretion scenario, in order to provide further arguments in the debate. By  $\dot{M}_{\text{accr}}$ , it is usually meant the accretion rate onto the central body, and this is our adopted viewpoint throughout this whole paper. In further more complete models, we will distinguish between the accretion from the molecular cloud to the disk and the accretion from the disk to the central protostar.

In Sect. 2, we examine some recent results on mass accretion and outflows in ultra-compact HII (UC HII) regions. In Sect. 3, we compare to the observations of pre-main sequence (PMS) stars some standard birthlines, i.e. with constant or slowly variable  $\dot{M}_{\text{accr}}$ . In Sect. 4, we calculate new birthlines with quickly increasing accretion rates. In Sect. 5, we briefly give our conclusions, and in particular we discuss the issue of the maximum stellar mass in the accretion paradigm.

---

Send offprint requests to: P. Norberg (peder.norberg@durham.ac.uk)

## 2. The accretion scenario for massive stars

The accretion scenario, despite its successes (Palla & Stahler, 1993), has been considered to be impossible for massive stars, due to their high luminosities, which are able to reverse the collapse (Bonnell et al. 1998; Stahler et al. 2000). In this case, the radiation pressure on the dust is high enough, so that its momentum can be transferred to the gas (Wolfire & Cassinelli, 1987). In the accretion scenario, the accretion rate  $\dot{M}_{\text{accr}}$  is an essential parameter, since it determines the momentum of the infalling material.

In their discussion on the study of the difficulties to form massive stars with the accretion scenario, Stahler et al. (2000) assume that the accretion rate behaves like

$$\dot{M}_{\text{accr}} \simeq \frac{c_s^3}{G} \quad (1)$$

where  $c_s$  is the sound speed in the molecular cloud. They stress that a remarkable property of this rate is that it is independent of the density of the parent cloud. The value of  $c_s$ , of course, depends very much on the temperature of the cloud. Stahler et al. (2000) assume that the pre-collapse temperature is independent of the core density and mass, and also suggest that this does not change too much, if the infalling material goes via a disk instead of landing directly on the stellar surface. With the assumption that clouds where massive stars form have the same typical temperature  $T = 10\text{--}20$  K as those where low mass stars form, Stahler et al. (2000) get accretion rates of  $10^{-5}$  to  $10^{-6} M_{\odot} \text{ yr}^{-1}$ . It is with this kind of assumptions that the constant accretion rates models by Beech & Mitalas (1994), and those with slowly varying accretion rates by Bernasconi & Maeder (1996) have been constructed. The birthline of these models joins the zero-age sequence when the heat released by the nuclear reactions stops the stellar contraction. This occurs typically around 8 to  $10 M_{\odot}$ .

For massive stars with accretion rates of the order of  $10^{-5} M_{\odot} \text{ yr}^{-1}$ , it is true that the momentum of the infalling material is much smaller than the outwards radiation momentum of the star, which is thus able to reverse the accretion process. Therefore such low mass accretion rates are impossible for massive stars. This is by the way also confirmed by the existence, around these massive stars, of stellar winds of similar magnitudes but blowing in the opposite direction. Moreover, we note that for this kind of  $\dot{M}_{\text{accr}}$  the formation lifetimes would be longer than the main sequence lifetime! The dynamics of the infalling material on protostars has been studied in detail by Wolfire & Cassinelli (1987). They found that the abundance of dust as well as the size of the grains should be reduced to allow infall. They examined the permitted regions in a plane  $\log \dot{M}_{\text{accr}}$  vs.  $\log M$ , where  $M$  is the mass of the newly formed star. E.g. for a star of  $40 M_{\odot}$ , the allowed region lies between  $\dot{M}_{\text{accr}} \simeq 10^{-4}$  and  $10^{-2} M_{\odot} \text{ yr}^{-1}$ . For lower  $\dot{M}_{\text{accr}}$ , the accretion is halted by the radiation field, while for higher  $\dot{M}_{\text{accr}}$  the total luminosity (the protostellar luminosity and the accretion induced shock luminosity) exceeds the Eddington luminosity.

There should be some relation between the accretion rates from collapsing clouds and their temperature  $T$  (Wolfire &

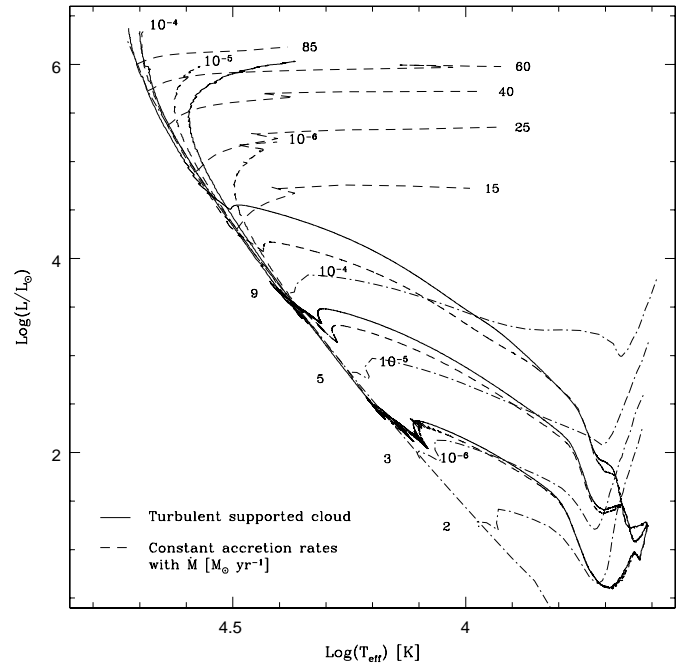


**Fig. 1.** Comparison between birthlines calculated with constant accretion rates and those calculated with expression 3, applied to the models by Bernasconi & Maeder (1996). The models are given for  $F = 0.1, 1.0$  and  $10.0$  and they correspond to about  $\dot{M}_{\text{cst}} = 10^{-6}, 10^{-5}$  and  $10^{-4} M_{\odot} \text{ yr}^{-1}$ . The dot-broken lines are the PMS tracks for constant mass with the indicated value (Bernasconi & Maeder, 1996). The tracks with broken lines in the upper part are post-Main Sequence (post-MS) tracks for massive stars of 15 to  $85 M_{\odot}$  by Schaller et al. (1992).

Cassinelli (1987)). However, this is true only if the thermal support is the only source of support in the clouds. In this case, which is likely not realistic, the temperature of the collapsing clouds leading to massive stars should be as high as  $T \geq 200$  K and maybe up to  $10^3$  K. This results from the expressions of the Jeans mass and the free fall timescale, which imply that the average inflow rate and the temperature of the collapsing cloud are increasing simultaneously.

There is a variety of results on the temperature of UC HII regions (Churchwell 1999 and Henning et al. 2000). From their infrared emission, Churchwell finds, around them, a sizeable ( $\sim 10^{16}$  cm) dust evacuated cavity and he estimates that the temperature at the inner face of the dust shell is typically 300 K. In the extreme case of W3, a massive star forming region, there is even a hard X-ray emission, implying  $T$  up to  $7 \cdot 10^7$  K in the wind-shocked cavity surrounding its central UC HII region (Hofner & Churchwell, 1997). The above results are likely to concern environments that have been altered by the presence of existing massive stars. Indeed, for the first stars to be formed one need to consider the temperature of the cloud core just before star formation begins. In regions like Orion, the so-called massive dense cores, which presumably are the birthsites of massive stars, are not as hot as the UC HII regions studied by Churchwell (1999) and Henning et al. (2000) indicate them to be. The temperature is more likely to be well below 100 K (Caselli & Myers 1995). Thus, the temperature of the molecular

**Table 1.** Birthline properties for accretion rate given by expr.4 with  $\varphi = 0.5$  and  $\dot{M}_{\text{ref}} = 10^{-5} M_{\odot} \text{yr}^{-1}$ . The columns are in general self explicit; however,  $M_{\text{core}}$  gives the convective core extension (in mass fraction),  $T_{\text{b}}$  is the temperature at the base of the convective envelope, when present; the surface content  ${}^2\text{H}_{\text{surf}}$  in deuterium and the central hydrogen content  ${}^1\text{H}_{\text{cent}}$  are both given in mass fraction.

NB	Age yr	Mass $M_{\odot}$	Log L $L_{\odot}$	Log $T_{\text{e}}$ K	dM/dt $M_{\odot} \text{yr}^{-1}$	$L_{\text{grav}}$ $L_{\odot}$	$M_{\text{core}}$ M/ $M_{\odot}$	Log $T_{\text{b}}$ K	${}^2\text{H}_{\text{surf}}$	${}^1\text{H}_{\text{cent}}$
1	0.000E+00	0.700	1.241	3.609	0.836E-06	17.36	1.000	5.832	5.00E-05	6.800E-01
2	3.271E+05	1.000	0.838	3.649	0.999E-06	4.70	1.000	6.250	5.68E-08	6.800E-01
3	1.156E+06	2.001	0.648	3.705	0.141E-05	1.22	0.000	6.474	4.87E-10	6.800E-01
4	1.791E+06	3.000	1.767	3.857	0.173E-05	55.02	0.000		4.20E-05	6.800E-01
5	2.327E+06	4.000	2.456	4.176	0.200E-05	133.86	0.132		1.10E-05	6.793E-01
6	2.799E+06	5.000	2.738	4.241	0.223E-05	-116.69	0.267		1.14E-05	6.780E-01
7	3.230E+06	6.011	3.077	4.294	0.244E-05	-145.66	0.249		5.00E-05	6.755E-01
8	3.628E+06	7.024	3.336	4.334	0.264E-05	-155.52	0.256		5.00E-05	6.730E-01
9	3.993E+06	8.022	3.489	4.362	0.282E-05	-171.74	0.291		5.00E-05	6.706E-01
10	4.341E+06	9.037	3.646	4.388	0.299E-05	-199.69	0.319		5.00E-05	6.677E-01
11	4.656E+06	10.008	3.790	4.411	0.315E-05	-219.64	0.335		5.00E-05	6.640E-01
12	5.301E+06	12.147	4.055	4.450	0.346E-05	-263.28	0.331		5.00E-05	6.538E-01
13	5.828E+06	14.047	4.247	4.478	0.372E-05	-301.07	0.356		5.00E-05	6.426E-01
14	6.355E+06	16.085	4.425	4.502	0.398E-05	-366.45	0.385		5.00E-05	6.315E-01
15	6.834E+06	18.058	4.572	4.522	0.422E-05	-426.49	0.411		5.00E-05	6.189E-01
16	7.313E+06	20.146	4.708	4.539	0.446E-05	-486.96	0.470		5.00E-05	6.024E-01
17	8.354E+06	25.080	4.974	4.568	0.499E-05	-646.14	0.465		5.00E-05	5.620E-01
18	9.305E+06	30.062	5.189	4.585	0.547E-05	-915.03	0.486		5.00E-05	5.052E-01
19	1.018E+07	35.073	5.375	4.595	0.591E-05	-1234.56	0.513		5.00E-05	4.564E-01
20	1.099E+07	40.028	5.530	4.590	0.632E-05	-1702.94	0.530		5.00E-05	3.818E-01
21	1.175E+07	45.018	5.670	4.569	0.670E-05	-2319.24	0.503		5.00E-05	2.939E-01
22	1.248E+07	50.009	5.798	4.512	0.706E-05	-3345.30	0.467		5.00E-05	1.699E-01
23	1.317E+07	55.012	5.923	4.395	0.741E-05	-2531.52	0.417		5.00E-05	2.512E-02

cloud is not necessarily the only parameter responsible for the enhanced accretion rates necessary to form massive stars.

In massive star forming regions, like Orion, the velocity width of an observed line is dominated by non-thermal, supersonic motions (e.g. Caselli & Myers 1995). Thus, there is a significant contribution of turbulent motions to the support of the clouds. In Eq. (1) for the accretion rate, the thermal sound speed should be replaced by the sum of a thermal and non-thermal contribution. Turbulence takes a long time to be dissipated and persists during a significant part of the formation process. Caselli & Myers (1995) find a higher density and pressure in massive cores leading to a fast mass infall. Thus, it may be that the turbulence and the higher density of the ambient gas favour higher accretion rates in massive star forming molecular clouds (we are indebted to Prof. F. Palla for this very important remark).

There are remarkable results concerning the presence of huge, likely bipolar, molecular outflows coming out of the regions of massive star formation. The luminosities of these regions are estimated from the radio free-free fluxes and/or from the integrated IR fluxes. The outflow rates come from the expansion velocities of the CO(1-0) line (Churchwell, 1999). The outflow rates  $\dot{M}_{\text{out}}$  behave continuously like  $L_{\text{bol}}^{0.7}$  over 6 decades of luminosity (Shepherd & Churchwell, 1996). Around the solar luminosity, the values of  $\dot{M}_{\text{out}}$  are about  $10^{-5} M_{\odot} \text{yr}^{-1}$ , i.e. of the same order as the currently estimated accretion rates. However for massive stars with L from  $10^4$  to  $10^6 L_{\odot}$ , the outflow

rates  $\dot{M}_{\text{out}}$  are in the range of  $10^{-3}$  to  $10^{-2} M_{\odot} \text{yr}^{-1}$ . There are several possible origins for these large outflows, however the review of the arguments by Churchwell (1999) favours the possibility that the massive outflows are driven by accretion, although it is not yet proved. From the large masses present in the outflows and the luminosity of the central object, he estimates that the fraction  $f$  of the infalling material incorporated into the star is about 15%, while 85% are deflected in the outflows. Adopting a mass-luminosity relation of the form  $L \sim M^3$ , Churchwell (1999) suggests that the outflow rates behave like  $\dot{M}_{\text{out}} \sim M^{2.1}$ . If we specifically consider, for example, the mass-luminosity relation from the models by Schaller et al. (1992) in the broad mass interval of 2 to  $85 M_{\odot}$ , we would get

$$\dot{M}_{\text{accr}} = 1.5 \cdot 10^{-5} f \left( \frac{M}{M_{\odot}} \right)^{1.54} M_{\odot} \text{yr}^{-1}, \quad (2)$$

where  $f$  is the accreted fraction of the infalling material. Such results suggests that constant accretion rates of the order of  $10^{-5} M_{\odot} \text{yr}^{-1}$  do not necessarily apply for all ranges of stellar masses and that much larger values of  $\dot{M}_{\text{accr}}$  may have to be considered for larger masses. If this is true, several of the arguments against the accretion scenario for massive stars may not apply.

We also note that there is a class of theoretical models of cloud equilibria which do in fact predict a strong dependence of the mass accretion rate on protostellar mass. These are the

**Table 2.** Same as in Table 1, but for  $\varphi = 1.0$ .

NB	Age yr	Mass $M_{\odot}$	Log L $L_{\odot}$	Log $T_e$ K	dM/dt $M_{\odot} \text{ yr}^{-1}$	$L_{\text{grav}}$ $L_{\odot}$	$M_{\text{core}}$ $M/M_{\odot}$	Log $T_b$ K	${}^2\text{H}_{\text{surf}}$	${}^1\text{H}_{\text{cent}}$
1	0.000E+00	0.700	1.241	3.609	0.700E-06	17.36	1.000	5.832	5.00E-05	6.800E-01
2	3.575E+05	1.000	0.793	3.649	0.999E-06	4.03	1.000	6.274	2.80E-08	6.800E-01
3	1.050E+06	2.001	0.666	3.704	0.199E-05	0.05	0.000	6.427	1.24E-09	6.800E-01
4	1.456E+06	3.000	1.558	3.802	0.299E-05	29.24	0.000		4.79E-05	6.800E-01
5	1.744E+06	4.002	2.776	4.197	0.399E-05	-33.63	0.197		1.04E-05	6.799E-01
6	1.967E+06	5.000	2.661	4.213	0.499E-05	89.33	0.211		1.05E-05	6.793E-01
7	2.149E+06	6.000	3.086	4.305	0.599E-05	-374.60	0.293		1.08E-05	6.783E-01
8	2.308E+06	7.031	3.280	4.331	0.699E-05	-425.53	0.276		5.00E-05	6.770E-01
9	2.445E+06	8.059	3.515	4.366	0.798E-05	-516.27	0.266		5.00E-05	6.756E-01
10	2.561E+06	9.046	3.680	4.393	0.896E-05	-564.90	0.278		5.00E-05	6.744E-01
11	2.667E+06	10.056	3.800	4.415	0.996E-05	-667.72	0.313		5.00E-05	6.735E-01
12	2.851E+06	12.073	4.034	4.452	0.119E-04	-880.94	0.359		5.00E-05	6.712E-01
13	3.005E+06	14.082	4.236	4.483	0.139E-04	-1084.87	0.365		5.00E-05	6.682E-01
14	3.141E+06	16.113	4.405	4.508	0.159E-04	-1159.10	0.412		5.00E-05	6.660E-01
15	3.257E+06	18.085	4.546	4.528	0.179E-04	-1623.84	0.439		5.00E-05	6.635E-01
16	3.363E+06	20.104	4.672	4.546	0.199E-04	-1725.76	0.466		5.00E-05	6.606E-01
17	3.586E+06	25.084	4.921	4.579	0.248E-04	-2599.08	0.503		5.00E-05	6.545E-01
18	3.769E+06	30.116	5.116	4.603	0.298E-04	-3324.35	0.566		5.00E-05	6.469E-01
19	3.924E+06	35.128	5.272	4.621	0.347E-04	-4241.38	0.606		5.00E-05	6.408E-01
20	4.059E+06	40.193	5.401	4.635	0.398E-04	-5319.48	0.640		5.00E-05	6.351E-01
21	4.175E+06	45.113	5.509	4.645	0.446E-04	-6289.63	0.669		5.00E-05	6.293E-01
22	4.278E+06	49.946	5.600	4.654	0.491E-04	-6833.45	0.656		5.00E-05	6.262E-01
23	4.376E+06	55.062	5.682	4.660	0.546E-04	-8946.76	0.715		5.00E-05	6.194E-01
24	4.466E+06	60.217	5.758	4.665	0.597E-04	-10319.23	0.686		5.00E-05	6.144E-01
25	4.622E+06	70.340	5.887	4.671	0.698E-04	-6300.715	0.718		5.00E-05	6.097E-01
26	4.753E+06	80.182	5.991	4.683	0.796E-04	-6455.416	0.739		5.00E-05	6.012E-01
27	4.977E+06	100.23	6.160	4.689	0.996E-04	-23297.530	0.768		5.00E-05	5.852E-01

so-called logatropic spheres studied by McLaughlin & Pudritz (1996, 1997) and Galli et al. (1999), where internal pressure varies like the logarithm of the density. The equation of state departs from isothermal, and the sound speed increases with decreasing density. These models are useful to account for the line width density relation observed for molecular clouds. The accretion rate onto a protostar is not constant in logatropic models, but grows like  $t^3$ , which implies that  $\dot{M}_{\text{accr}}$  varies like  $M^{\frac{3}{4}}$  (McLaughlin & Pudritz 1997). These models have also been applied to study the collapse of hot molecular cores leading to the formation of massive stars (Osorio et al. 1999).

In view of all the above arguments in favour of possible large accretion rates, we do think it is worth to further examine the accretion scenario for the formation of massive stars.

### 3. Simple birthlines with constant or slowly varying accretion

In this section, we briefly show for the purpose of comparison some new sets of birthlines obtained with constant and slowly varying  $\dot{M}_{\text{accr}}$ . The initial quasi-static model with a mass  $M_{\text{ini}} = 0.7 M_{\odot}$  are fully convective (see Stahler 1988; Bernasconi & Maeder, 1996) and are started before the deuterium-burning sequence, which is treated with a time dependent convection scheme. It is well known that the initial D-abundance and that

of the accreting matter influence the PMS evolution; here the initial and cosmic D abundance is taken  $5 \cdot 10^{-5}$  in mass fraction consistently with the results by Geiss (1993). From many test models by Bernasconi & Maeder (1996), it appears that the exact value chosen for the initial model has no significant influence for the PMS structure and on the evolution of intermediate and massive stars. Only the age is possibly influenced by this choice (see comments made about Tables 1, 2 and 3 below).

#### 3.1. Constant values of $\dot{M}_{\text{accr}}$

Our simplest accretion model considers a constant mass accretion rate. In a recent study of the Orion Nebula, Palla & Stahler (1999) have used constant values  $\dot{M}_{\text{accr}}$  equal to  $10^{-5} M_{\odot} \text{ yr}^{-1}$ . In Fig. 1, the birthlines corresponding to  $\dot{M}_{\text{accr}}$  to  $10^{-6}$ ,  $10^{-5}$  and  $10^{-4} M_{\odot} \text{ yr}^{-1}$  are shown. Higher accretion rates lead to birthlines with higher luminosities. For high accretion rates, a star gains more mass and thus luminosity during its PMS contraction and reaches the ZAMS at a higher luminosity. Deuterium is also continuously brought to the star and contributes to the stellar luminosity (cf. Bernasconi & Maeder, 1996). Tout et al. (1999) have recently shown that the PMS tracks and age estimates of PMS stars are very much influenced by the accretion rates and this is indeed in agreement with the present results.

**Table 3.** Same as in Table 1, but for  $\varphi = 1.5$ .

NB	Age yr	Mass $M_{\odot}$	Log L $L_{\odot}$	Log T <sub>e</sub> K	dM/dt $M_{\odot} \text{ yr}^{-1}$	L <sub>grav</sub> $L_{\odot}$	M <sub>core</sub> M/ $M_{\odot}$	Log T <sub>b</sub> K	<sup>2</sup> H <sub>surf</sub>	<sup>1</sup> H <sub>cent</sub>
1	0.000E+00	0.700	1.241	3.609	0.585E-06	17.36	1.000	5.832	5.00E-05	6.800E-01
2	3.907E+05	1.000	0.745	3.649	0.999E-06	3.42	1.000	6.297	1.46E-08	6.800E-01
3	9.767E+05	2.000	0.721	3.708	0.282E-05	-1.22	0.000	6.129	5.89E-06	6.800E-01
4	1.236E+06	3.000	1.120	3.766	0.519E-05	7.92	0.000	6.065	1.68E-05	6.800E-01
5	1.391E+06	4.002	2.548	4.067	0.799E-05	340.19	0.000		2.11E-05	6.800E-01
6	1.496E+06	5.000	3.018	4.268	0.111E-04	-476.96	0.350		1.13E-05	6.797E-01
7	1.574E+06	6.000	2.944	4.266	0.146E-04	-1851.30	0.454		1.12E-05	6.794E-01
8	1.635E+06	7.001	3.297	4.342	0.185E-04	-1275.61	0.340		1.17E-05	6.790E-01
9	1.684E+06	8.004	3.560	4.369	0.226E-04	-1535.61	0.263		5.00E-05	6.784E-01
10	1.725E+06	9.038	3.774	4.402	0.269E-04	-1468.14	0.255		5.00E-05	6.778E-01
11	1.760E+06	10.053	3.829	4.419	0.311E-04	-2105.96	0.288		5.00E-05	6.773E-01
12	1.818E+06	12.164	4.065	4.457	0.413E-04	-3042.56	0.335		5.00E-05	6.766E-01
13	1.857E+06	13.961	4.220	4.484	0.508E-04	-3639.83	0.359		5.00E-05	6.760E-01
14	1.896E+06	16.185	4.395	4.511	0.632E-04	-5075.49	0.423		5.00E-05	6.757E-01
15	1.925E+06	18.220	4.538	4.532	0.754E-04	-6693.96	0.460		5.00E-05	6.751E-01
16	1.949E+06	20.222	4.662	4.550	0.880E-04	-8078.64	0.484		5.00E-05	6.746E-01
17	1.997E+06	25.350	4.915	4.585	0.123E-03	-12403.20	0.535		5.00E-05	6.732E-01
18	2.031E+06	30.187	5.099	4.609	0.159E-03	-17836.61	0.577		5.00E-05	6.721E-01
19	2.060E+06	35.516	5.261	4.629	0.203E-03	-24182.66	0.616		5.00E-05	6.711E-01
20	2.079E+06	39.887	5.372	4.642	0.241E-03	-30703.26	0.644		5.00E-05	6.704E-01
21	2.099E+06	45.110	5.485	4.655	0.289E-03	-39344.84	0.672		5.00E-05	6.697E-01
22	2.113E+06	49.724	5.571	4.664	0.333E-03	-47801.27	0.697		5.00E-05	6.692E-01
23	2.128E+06	55.077	5.658	4.673	0.388E-03	-58971.57	0.718		5.00E-05	6.685E-01
24	2.142E+06	61.335	5.746	4.681	0.454E-03	-72931.53	0.737		5.00E-05	6.679E-01
25	2.161E+06	71.464	5.869	4.691	0.569E-03	-98576.05	0.767		5.00E-05	6.670E-01
26	2.176E+06	80.783	5.964	4.699	0.682E-03	< -1.0E+05	0.796		5.00E-05	6.664E-01
27	2.200E+06	100.86	6.128	4.710	0.945E-03	< -1.0E+05	0.833		5.00E-05	6.653E-01

### 3.2. Slowly varying $\dot{M}_{\text{accr}}$

The models by Bernasconi & Maeder (1996) did not use constant accretion rates, but the values of  $\dot{M}_{\text{accr}}$  were slightly increasing with the already accreted mass, according to the prescriptions of a simple model of collapsing clouds. This model needs several input parameters such as the temperature T of the cloud (currently 30 K), the mean molecular weight  $\mu$  (currently 2.4). The effect of turbulent pressure were accounted for according to the velocity dispersion vs. size of the clouds given by Larson (1981). In Fig. 1, a model with these prescriptions is also shown (model with F=1.0). We also show two other models with rates 10 times smaller and 10 times larger than the rates  $\dot{M}_{\text{BM}}$  by Bernasconi & Maeder (1996), according to the expression

$$\dot{M}_{\text{accr}} = F \dot{M}_{\text{BM}} \quad (3)$$

Fig. 1 indicates clearly the differences between the two sets of models. These differences are small, especially for the low accretion rates. The model with F=0.1 reaches the ZAMS at about 4.4  $M_{\odot}$ , the one with F=1.0 at 9.5  $M_{\odot}$ , and at 27.5  $M_{\odot}$  for F = 10.0. After having reached the ZAMS, the continuously accreting protostar carries on its evolution along the ZAMS.

On the upper main sequence, the tracks are also influenced by the accretion rates. For low  $\dot{M}_{\text{accr}}$ , the time necessary to build up a massive star is so long that the star begins to burn a

large fraction of its central hydrogen. Thus it has already moved away from the ZAMS, when it becomes visible at the end of its very long accretion phase. For high accretion rates, the time necessary to form a massive star is so short that a small amount of hydrogen is burnt and therefore the star becomes visible close to the ZAMS. These features are well shown in Fig. 1.

In Fig. 2, we compare 12 birthlines made with F values between 0.1 and 5.0 with recent observations of PMS stars in various clusters (the references are given in the figure caption). Indications are given for stars which have observed values of the accretion rates. Let us note with caution that there are considerable uncertainties in the derivations of luminosities and T<sub>eff</sub>, as shown by the error bars. The birthlines have to be seen as upper envelopes, since a fraction of the stars may already have ended their accretion phase and are moving towards the ZAMS along the canonical PMS tracks. We do not know whether one single birthline should apply to various star groups; however let us for simplicity adopt such a view.

From Fig. 2, we can make the following remarks. –1. A birthline with F between 1 and 5 fits best as an upper envelope, this corresponding to  $\dot{M}_{\text{accr}}$  in the range of  $10^{-5}$  and  $10^{-4} M_{\odot} \text{ yr}^{-1}$ . Thus, it is very likely that accretion rates higher than the currently used values of  $10^{-5} M_{\odot} \text{ yr}^{-1}$  are necessary, at least for the most luminous PMS stars. –2. The upper part of the tracks at the time the star becomes visible also depends on the previous

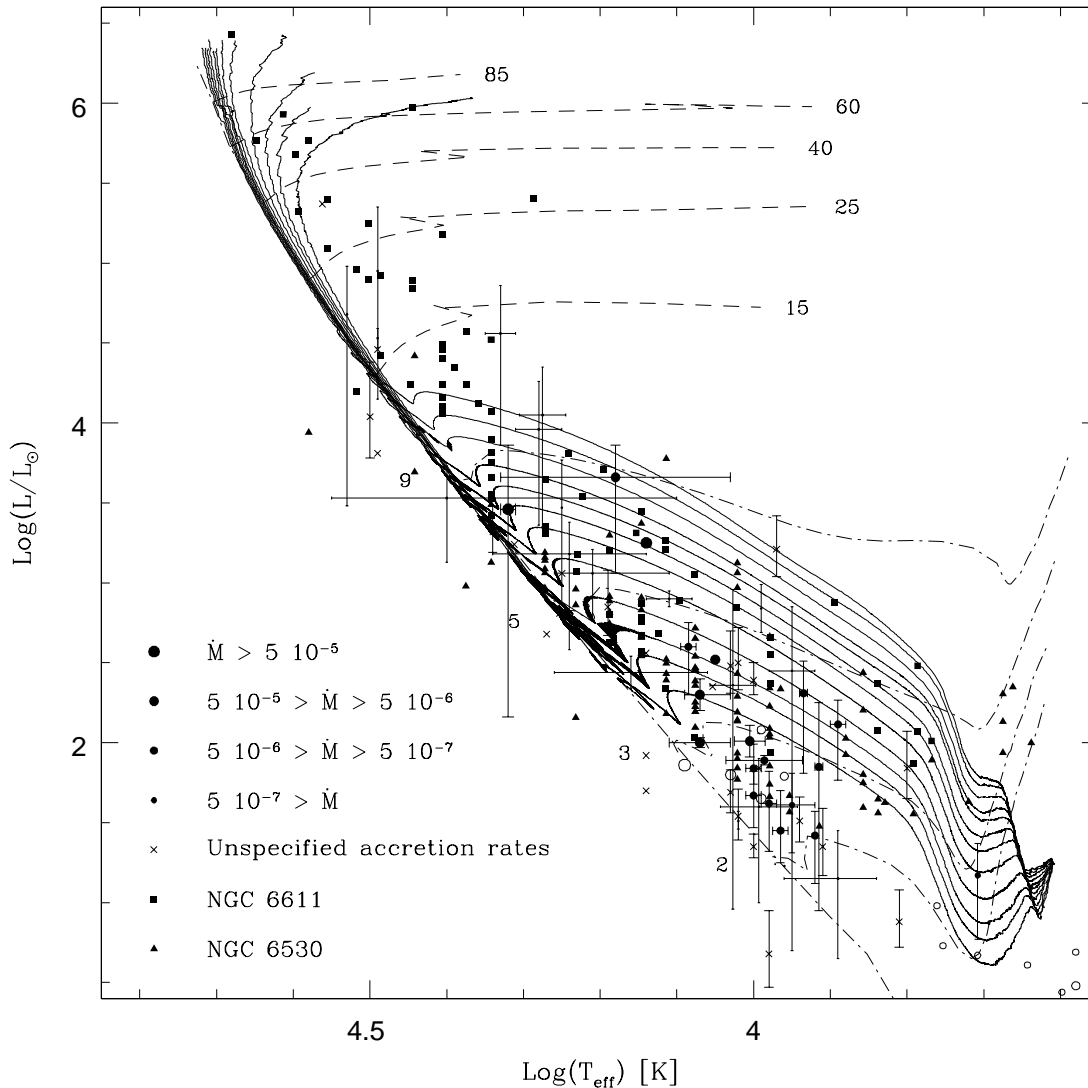


**Fig. 2.** This grid of birthlines (continuous lines) is made out of twelve tracks with the following values of  $F = 0.1, 0.15, 0.2, 0.3, 0.5, 0.75, 1.0, 1.25, 1.75, 2.5, 3.5, 5.0$ . In general, the luminosity increases with  $F$  for a fixed value of the effective temperature. Pre-main sequence evolution tracks with constant mass are in dot-broken lines (Bernasconi & Maeder, 1996) and the post-main sequence tracks from Schaller et al. (1992) are in short dashed lines. The labels correspond to the mass along each track. Observations are issued from: 1. compilation done by Bernasconi & Maeder (1996); 2. Hillenbrand et al. (1992); 3. Damiani et al. (1994); 4. Cohen & Kuhl (1979); 5. van den Ancker et al. (1997a); 6. Berrilli et al. (1992); 7. de Winter et al. (1997); 8. Thé et al. (1990); 9. van den Ancker et al. (1998); 10. van den Ancker et al. (1997b). For those stars with an error estimate on the luminosity and/or the effective temperature, the error bars are plotted. Moreover if several measures exist for a same star, we give the average value and indicate the existing dispersion on it. The value of  $\dot{M}_{\text{accr}}$  is given by the size of the symbol, and an open symbol signifies that several groups have measured  $L$  and  $T_{\text{eff}}$  for this star.

accretion rates (Figs. 1 and 3). There is some support towards high  $\dot{M}_{\text{accr}}$  from the observations by Hanson et al. (1997). They find some very massive PMS objects ( $M \geq 60 M_{\odot}$ ) close to the ZAMS and as seen above this also constrains the accretion rates. Thus these stars have to be formed in a time of the order of  $10^6$  yr at most. This implies an *average* accretion rate of about  $10^{-4} M_{\odot} \text{ yr}^{-1}$ . Thus, a most critical difficulty for all these birthlines with slowly increasing  $\dot{M}_{\text{accr}}$  is their too long lifetimes (cf. also Hanson et al. 1997). -3. The observations suggest that the birthline should join the ZAMS between about 9 and  $15 M_{\odot}$ . -4. The distribution of stars in the HR diagram do not tightly

constrain the slope of the birthline. However, we note that the observed distribution of stars in Fig. 2 seems to suggest a slope, which may be steeper than the one predicted by Bernasconi & Maeder (1996). Especially the birthline could be lower at lower luminosities.

The various difficulties met with these accretion models as a formation mechanism of massive stars lead us to examine in the next section models where the accretion rate  $\dot{M}_{\text{accr}}$  increases more rapidly with mass. Indeed this will give rise to birthlines with steeper slopes in the HR diagram and at the same time shorten the formation timescales.

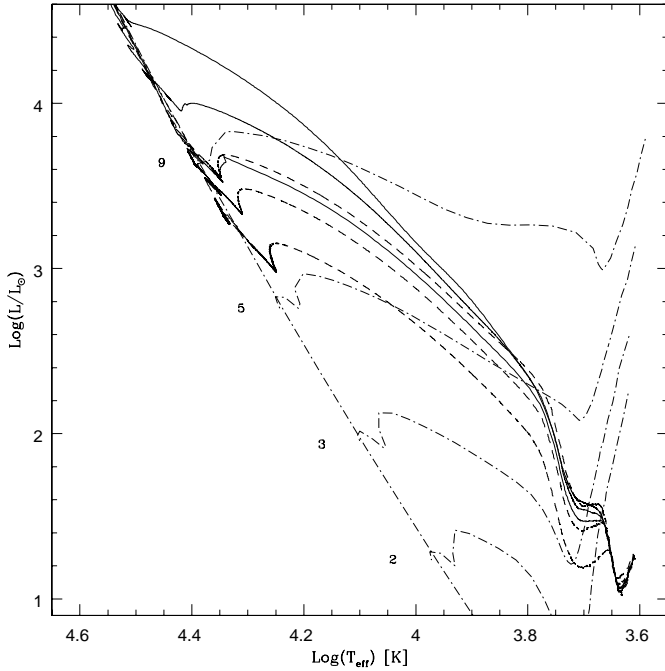


**Fig. 3.** The continuous lines show the tracks calculated with expr. 4 for  $\dot{M}_{\text{ref}} = 10^{-5}$  and for  $\varphi = 1.5, 1.0$  and  $0.5$  from top to bottom. The broken lines are the birthlines calculated with expression 3 and  $F = 0.5, 1.0$  and  $1.5$ . The dot-broken lines are the PMS tracks for constant mass with the indicated value (Bernasconi & Maeder 1996).

#### 4. Models with strongly increasing accretion rates

The results of the two previous sections suggest that the accretion rates may increase relatively quickly with the stellar mass. To further test this hypothesis, we examine the consequences of a power law with exponent  $\varphi$

$$\dot{M}_{\text{accr}}(M) = \dot{M}_{\text{ref}} \left( \frac{M}{M_{\odot}} \right)^{\varphi} \quad (4)$$

We consider that the accretion rate is increasing with an exponent  $\varphi$  of the mass. Models with  $\varphi = 0.5, 1.0$  and  $1.5$  are calculated. We provide in the Tables 1, 2 and 3 some important data for these models, assuming a reference mass loss rate  $\dot{M}_{\text{ref}}$  of  $10^{-5} M_{\odot} \text{ yr}^{-1}$ . We shall also test this value below. The models are started with an initial mass  $M_{\text{ini}} = 0.7 M_{\odot}$  and the zero of the age scales are placed at this time. Another possible choice (Bernasconi, 1996) would be to take as initial age  $\frac{0.7 M_{\odot}}{\langle \dot{M}_{\text{accr}} \rangle}$ , where  $\langle \dot{M}_{\text{accr}} \rangle$  represents the average accretion rate since the start of the formation process. As a matter of fact, we do not strictly know the zero point in the age scale, and therefore any convention is slightly arbitrary.

Fig. 3 shows 3 birthlines obtained with expression 4. We notice that the tracks by Bernasconi & Maeder (1996; corresponding to  $F = 1.0$ ) are rather close to those with  $\varphi = 0.5$ . For higher values of  $\varphi$ , we obtain, as expected, a much steeper slope of the birthlines. As shown in the Tables 1, 2 and 3, the models with a higher  $\varphi$  have much shorter formation times. In models of high  $\varphi$  the central H-content is still much higher, and the

size of their convective cores are larger. Both points are consistent with the fact that the ages are shorter and the evolution much less advanced. For  $\varphi = 0.5$ , and even more for the constant  $\dot{M}_{\text{accr}}$ , the PMS lifetimes  $t_{\text{PMS}}$  are longer than the Main Sequence (MS) lifetimes  $t_{\text{MS}}$  for massive stars above about  $20 M_{\odot}$ . In this case,  $t_{\text{MS}} = 8.1 \cdot 10^6 \text{ yr}$ , and  $t_{\text{PMS}} = 7.3 \cdot 10^6 \text{ yr}$ . This is a very severe problem for slowly increasing  $\dot{M}_{\text{accr}}$  and a very important argument in favour of models with an accretion rate quickly increasing with stellar mass. For  $\varphi = 1.0$ , the equality of the two lifetimes  $t_{\text{PMS}}$  and  $t_{\text{MS}}$  is realized around a mass of about  $45 M_{\odot}$ ; however a large fraction of  $t_{\text{PMS}}$  is still spent in the low mass regime.

For  $\varphi = 1.5$ , the situation with respect to the lifetimes is much more satisfactory, as  $t_{\text{PMS}}$  is shorter than  $t_{\text{MS}}$  up to at least  $120 M_{\odot}$ . Moreover, half of  $t_{\text{PMS}}$  is spent below a mass of  $2 M_{\odot}$ , and the time for the star to evolve from  $2$  to  $120 M_{\odot}$  is about  $10^6 \text{ yr}$ , which is an acceptable value. Due to this we must stress that accretion rates strongly increasing with mass become a necessity in order to form stars on a timescale significantly smaller than the MS lifetime, so that they have not evolved too far from the ZAMS when they become visible. Also, a too long lifetime will allow a massive star to ionize a too large surrounding region, preventing any further accretion. In this respect, we emphasize that the models with  $\varphi \simeq 1.5$  are much more favourable than the other ones studied here.

These calculations raise the question whether, at a given value of the stellar mass, the initial formation of a massive star occurs with the same accretion rate as for a star with a low final mass. This is what is assumed here. This looks reasonable, since according to Newton's Theorem the gravitational potential in a spherical configuration is determined by the matter within the considered radius. However, further studies may show the importance of environmental effects, such as the local density and temperature in a cluster, which are not taken into account in the present study.

In order to further examine the accretion rates and their dependence on  $\varphi$  and  $\dot{M}_{\text{ref}}$  in expr. 4, some other models have been calculated. Fig. 4 shows models for  $\varphi = 1.0$  and  $\dot{M}_{\text{ref}} = 10^{-6}, 2 \cdot 10^{-6}, 5 \cdot 10^{-6}$  and  $10^{-5} M_{\odot} \text{ yr}^{-1}$  respectively. These birthlines are compared to the observations already shown in Fig. 2. Clearly the highest value for  $\dot{M}_{\text{ref}}$  gives the best fit as an upper envelope. This confirms that in the range of intermediate mass stars the accretion rates are not as low as  $10^{-5} M_{\odot} \text{ yr}^{-1}$ . As already noticed for Fig. 2, it is difficult to obtain constraints on the slope  $\varphi$  from the point distributions in the HR diagram. However, the agreement for the highest curve in Fig. 4 is rather better than for Fig. 2. Also, it is possible that the theoretical slope is not steep enough in view of the observations. From the envelopes in the HR diagram, the values of  $\dot{M}_{\text{ref}}$  are much better determined than the value of  $\varphi$ .

Fig. 5 shows the same kind of results, but for an exponent  $\varphi = 1.5$  and  $\dot{M}_{\text{ref}} = 10^{-6}, 5 \cdot 10^{-6}$  and  $10^{-5} M_{\odot} \text{ yr}^{-1}$  respectively. Clearly the two upper curves give the best fit, and maybe the highest one is the best. From the envelope fits in the HR diagram, it is hard to say whether a value  $\varphi = 1.0$  or  $1.5$  is best, however from the considerations on the lifetimes, the case with  $\varphi = 1.5$  is

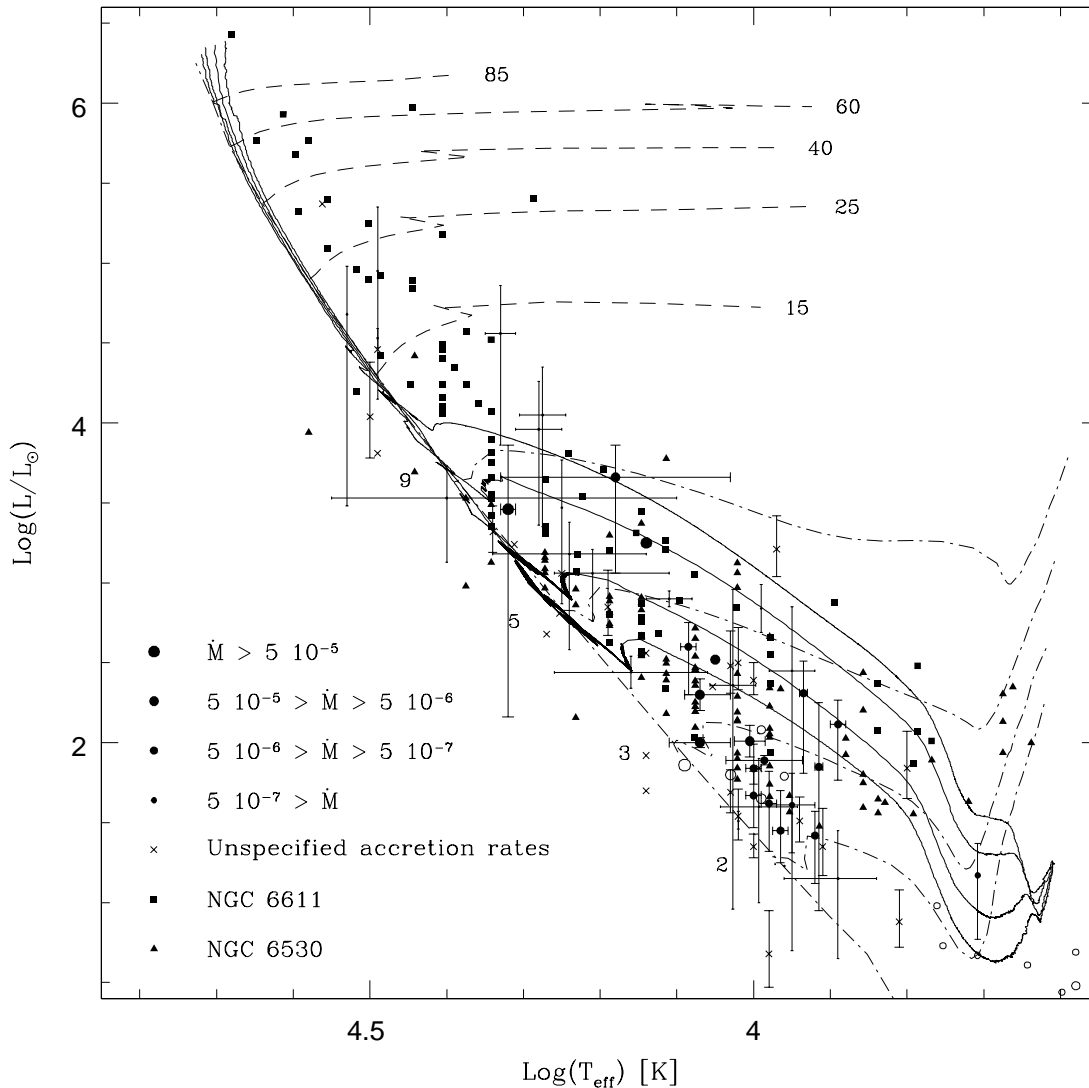


**Fig. 4.** The continuous lines represent birthlines obtained with  $\varphi = 1.0$  and  $\dot{M}_{\text{ref}}$  being equal to  $10^{-6}$ ,  $2 \cdot 10^{-6}$ ,  $5 \cdot 10^{-6}$  and  $10^{-5} M_{\odot} \text{ yr}^{-1}$  from bottom to top respectively. The higher  $\dot{M}_{\text{ref}}$  is the higher the birthline is in the HR diagram. The other curves have the same meaning as in Fig. 2 and the observations are the same.

clearly favoured. Therefore, our preferred choice of parameters for the model given by expr. 4 is an exponent  $\varphi \simeq 1.5$  and a multiplying factor  $\dot{M}_{\text{ref}} \simeq 10^{-5} M_{\odot} \text{ yr}^{-1}$ .

We notice that it is amazing how this slope and the multiplying factor are close to the results obtained by Churchwell (1999) and Henning et al. (2000) and in particular to the values given in expr. 2. Without saying that the physical behaviour of the accretion rates is determined by a law which is exactly of the form given by expr. 4, it is interesting that these two very different approaches give a rather similar dependence with respect to the stellar mass. Further theoretical and observational analyses are needed to give more insight into the dependence of the accretion rate on various possible parameters.

## 5. Conclusions and remarks on the maximum stellar mass

The main result of this work is that the accretion rate of a forming protostar strongly depends on the protostar's mass. A birthline described by a power law

$$\dot{M}_{\text{accr}} = \dot{M}_{\text{ref}} \left( \frac{M}{M_{\odot}} \right)^{\varphi} \quad (5)$$

with  $\dot{M}_{\text{ref}} \simeq 10^{-5}$  and  $\varphi = 1.5$  gives the best upper envelope for PMS stars in the HR diagram and, more importantly, it satisfies also the constraints coming from the formation lifetimes. The above law is also quite consistent with radio and IR studies of protostellar outflows (Churchwell, 1999; Henning et al., 2000), which show  $\dot{M}_{\text{accr}}$  quickly increasing with the luminosity of the UC HII region.

It is interesting that the high values of  $\dot{M}_{\text{accr}}$  suggested here well correspond to the permitted domain of accretion rates found

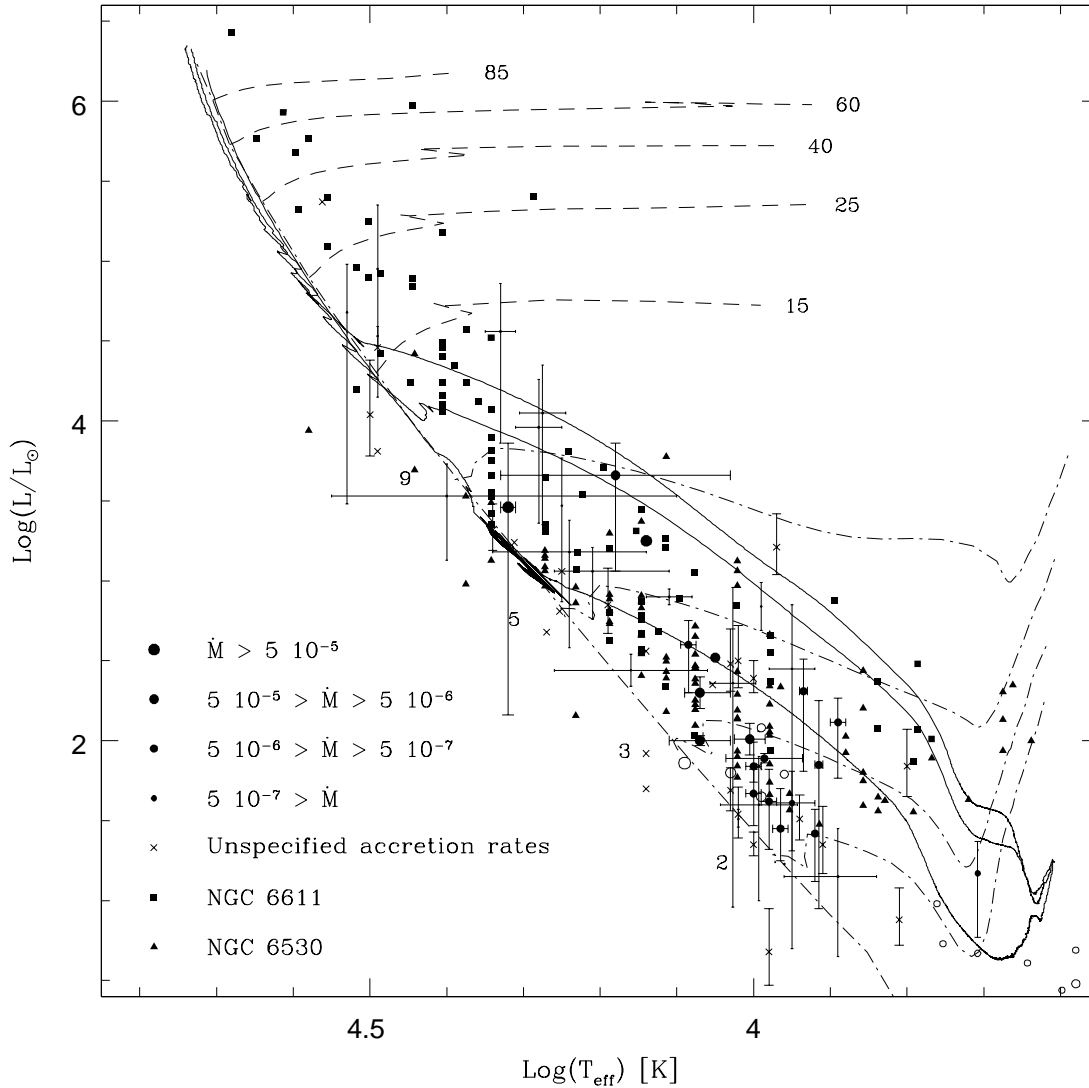


**Fig. 5.** The continuous lines represent birthlines obtained with  $\varphi = 1.5$  and  $\dot{M}_{\text{ref}}$  being equal to  $10^{-6}$ ,  $5 \cdot 10^{-6}$  and  $10^{-5} M_{\odot} \text{yr}^{-1}$  respectively. Same remarks as for Fig. 4

by Wolfire & Cassinelli (1987). The limits of this permitted domain are defined, on the low side of the values of  $\dot{M}_{\text{accr}}$ , by the condition that the momentum in the accretion flow is larger than the outwards radiation momentum. On the high side, it is fixed by the condition that the shock luminosity due to the accretion process is smaller than the Eddington luminosity. In addition, Wolfire & Cassinelli (1987) also found, for the occurrence of inflows onto massive stars, that the dust abundance has to be reduced by at least a factor of 4 and that the larger graphite grains are absent from the dust distribution function. In the context of the star models presented here, which do not follow the properties of the surrounding interstellar matter, we do not know whether this additional condition is met.

If this accretion scenario for forming massive stars proves to be the correct one, it has several further implications: on the luminosities and  $T_{\text{eff}}$  of the progenitors of massive stars; on the lifetimes of PMS evolution; on the initial stellar structure on the

ZAMS; on surface abundances of light elements; etc... It has also an impact on the slope of the initial mass function (IMF), since the final mass spectrum is not only shaped by the size of the collapsing fragments, which determine the reservoir of matter potentially available, but also by the accretion process which leads the star to reach its final mass.

Moreover the maximum stellar mass is determined by the physics intervening in the accretion process. In particular, the maximum stellar mass is the mass for which the accretion rate  $\dot{M}_{\text{accr}}$  is such that the shock luminosity  $L_{\text{shock}}$  due to the accretion plus the protostellar luminosity  $L_*$  is equal to the Eddington luminosity  $L_{\text{Edd}}$ , i.e.  $L_{\text{shock}} + L_* = L_{\text{Edd}}$ . If  $R_{\text{shock}}$  is the radius where the shock occurs, one has:

$$\frac{G\dot{M}_{\text{accr}}M}{R_{\text{shock}}} + L_* = \frac{4\pi cGM}{\kappa_{\text{dust}}}. \quad (6)$$

The relevant opacity to be considered here is the dust opacity  $\kappa_{\text{dust}}$  near the inner face of the dust cavity, since the grain opacity is the largest opacity source which may prevent further material accretion. As shown by Pollack et al. (1994), the main opacity source are organics below the vaporization temperature ( $T \simeq 500$  K) and silicates and metallic iron at higher temperatures. The opacity to be considered is likely the Planck opacity, i.e. the flux weighted opacity appropriate for small optical depths. The typical values of the Planck opacity  $\kappa_{\text{dust}}$  range between 2 and 8 cm<sup>2</sup>/g. Now, for the high accretion rates considered in the upper mass range, the shock luminosity dominates over the stellar luminosity by about 3 to 4 orders of magnitudes so that we may ignore  $L_*$ . Thus, we obtain a simple expression for the limiting accretion rate

$$\dot{M}_{\text{accr}} = \frac{4\pi c R_{\text{shock}}}{\kappa}. \quad (7)$$

If we consider for simplicity that the shock radius is some multiple  $\alpha$  of the stellar radius, we can apply the mass-radius relation obtained from the models of Schaller et al. (1992). The relation, valid between 40 and 120  $M_{\odot}$ , is thus:

$$\frac{R_{\text{shock}}}{R_{\odot}} = \alpha \left( \frac{M}{M_{\odot}} \right)^{0.557} \quad (8)$$

Now, we search for the intersection of the expression (5) for  $\dot{M}_{\text{accr}}(M)$  with relation (7) also accounting for (8). This gives the maximum possible stellar mass

$$\frac{M_{\text{shock}}}{M_{\odot}} = \left( \frac{41.6 \alpha}{\kappa_{\text{dust}}} \right)^{1.06} \quad (9)$$

with  $\kappa_{\text{dust}}$  expressed in cm<sup>2</sup>/g. The main interest is to emphasize that in the present context the maximum mass is defined by the intersection of  $\dot{M}_{\text{accr}}(M)$  with the accretion rate (7) giving a shock luminosity equal to the appropriate Eddington luminosity. More detailed models of the stellar surroundings are of course necessary. The above simple derivation may at most give an order of magnitude, if we know both the location of  $R_{\text{shock}}$  given by  $\alpha$  and  $\kappa_{\text{dust}}$ . While the approximate range of values of  $\kappa_{\text{dust}}$  is known as seen above, the value of  $\alpha$  is uncertain, since it depends on the adopted structure and turbulence of the clouds (cf. Pollack et al., 1994). As an example with  $\alpha \simeq 10$ , we would have a maximum mass between 70 and 300  $M_{\odot}$ .

The accretion scenario thus leads to a new simple concept for the maximum stellar mass. A change of metallicity will influence both the opacity and the location of the shock radius, thus the resulting effect of metallicity cannot be estimated without detailed models of collapsing clouds.

*Acknowledgements.* The authors want to express their gratitude to Prof. F. Palla for his most useful remarks on the manuscript. They also express their thanks to Dr. Georges Meynet for his advice and helpful discussions.

## References

- Beech M., Mitalas R., 1994, ApJS 95, 517  
 Bernasconi P.A., 1996, A&AS 120, 57  
 Bernasconi P.A., Maeder A., 1996, A&A 307, 829  
 Berrilli F., Corcuilo G., Ingrassio G., et al., 1992, ApJ 398, 254  
 Bonnell I.A., Bate M.R., Zinnecker H., 1998, MNRAS 298, 93  
 Caselli P., Myers P.C., 1995, ApJ 446, 665  
 Churchwell E., 1999, Massive Star Formation: The Role of Bipolar Outflows, in: Livio M. (ed.), Unsolved Problems in Stellar Evolution, Proc. STScI Meeting, in press  
 Cohen M., Kuhl L.V., 1979, ApJS 41, 743  
 Damiani F., Micela G., Sciortino S., et al., 1994, ApJ 436, 807  
 de Winter D., Koulis C., Thé P.S., et al., 1997, A&AS 121, 223  
 Galli D., Lizano S., Li Z.Y., et al., 1999, ApJ 521, 630  
 Geiss J., 1993, in: Prantzos N., Vangioni-Flam E., Cass M. (eds.), Origin and Evolution of the Elements, Cambridge: Univ. Press, p. 89  
 Hanson M.M., Howarth I.D., Conti P.S., 1997, ApJ 489, 698  
 Henning Th., Schreyer K., Launhardt R., et al., 2000, A&A 353, 211  
 Hillenbrand L.A., Strom S.E., Vrba F.J., et al., 1992, ApJ 397, 613  
 Hofner P., Churchwell E., 1997, ApJ 486, L39  
 Larson R.B., 1981, MNRAS 145, 271  
 McLaughlin D.E., Pudritz R.E., 1996, ApJ 469, 194  
 McLaughlin D.E., Pudritz R.E., 1997, ApJ 476, 750  
 Osorio M., Lizano S., D'Alessio P., 1999, ApJ 525, 808  
 Palla F., Stahler S.W., 1993, ApJ 418, 414  
 Palla F., Stahler S.W., 1999, ApJ 525, 772  
 Pollack J.B., Hollenbach D., Beckwith S., et al., 1994, ApJ 421, 615  
 Schaller G., Schaerer D., Meynet G., et al., 1992, A&AS 96, 269  
 Shepherd D.S., Churchwell E., 1996, ApJ 472, 225  
 Stahler S.W., 1988, ApJ 332, 804  
 Stahler S.W., Palla F., Ho P.T., 2000, in: Mannings V., et al. (eds.), Protostars and Planets IV. Tucson: Univ. of Arizona Press  
 Stahler S.W., Shu F.H., Taam R.E., 1981, ApJ 248, 727  
 Stahler S.W., Shu F.H., Taam R.E., 1980a, ApJ 241, 637  
 Stahler S.W., Shu F.H., Taam R.E., 1980b, ApJ 242, 226  
 Thé P.S., de Winter D., Feinstein A., et al., 1990, A&AS 82, 319  
 Tout C.A., Livio M., Bonnell I.A., 1999, MNRAS 310, 360  
 van den Ancker M.E., de Winter D., Tjin A Djie H.R.E., 1998, A&A 330, 145  
 van den Ancker M.E., Thé P.S., Tjin A Djie H.R.E., et al., 1997a, A&A 324, L33  
 van den Ancker M.E., Thé P.S., Feinstein A., et al., 1997b, A&AS 123, 63  
 Wolfire M.G., Cassinelli J.P., 1987, ApJ 319, 850